Kinematics of Overhanging Slopes in Discontinuous Rock

Michael Tsesarsky, Ph.D.[1]; and Yossef H. Hatzor, Ph.D., M.ASCE[2]

Abstract: The kinematics of overhanging rock slopes and the mechanical constraints associated with this specific slope geometry were studied. Investigation of the problem began with a generalized rigid body analysis and was followed by a numerical discontinuous deformation analysis, both of which were performed in two dimensions. It was found that eccentric loading and hence the development of tensile stresses at the base of overhanging rock slopes control their stability. Global slope instability, which is typically manifested in a forward rotation failure mode, may ensue if a through-going vertical discontinuity, typically referred to as "tension crack," transects the slope at the back. The transition from stable to unstable configurations depends on the distance between the tension crack and the toe of the slope. On the basis of the analysis, a simple threefold stability classification—stable, conditionally stable, and unstable—is proposed. In addition, geometrical guidelines, based on standard field mapping data, for the above stability classification are provided. Finally, the optimal reinforcement strategy for overhanging slopes is explored. The stability of overhanging slopes is determined by their eccentricity ratio, defined by the ratio between the base (B) and top (L) lengths: $e_r=B/L$. It was found that an overhanging slope with eccentricity ratio of $e_r<0.38$ is unstable and requires reinforcement. With an eccentricity ratio between $0.38<e_r<0.62$, the slope is considered conditionally stable against toppling failure, and reinforcement should be considered if the geometry approaches the lower bound eccentricity of 0.38. A comparison of full and partial face reinforcement schemes showed that full face reinforcement is preferable. The findings of this study were demonstrated by using an illustrative case study in which the stability of a 34 m high overhanging slope in a highly discontinuous rock mass was studied and an optimal rock bolt reinforcement scheme was designed.

DOI: 10.1061/(ASCE)GT.1943-5606.0000049

CE Database subject headings: Slope stability; Kinematics; Eccentric loads; Rocks; Bolts; Geometry.

Introduction

Rotational instabilities in rock slopes are generally attributed to the intersection of steeply inclined and gently dipping discontinuities, forming columns of massive rock blocks resting on a basal detachment surface (Fig. 1). If these columns lean against the rock, "back slumping" may occur (Kieffer 1998; Wittke 1965) [Fig. 1(a)]. If, on the other hand, these columns lean toward the excavation space, toppling may occur (Goodman and Bray 1976).

Adikahry et al. (1997), following Goodman and Bray (1976) and Evans (1981), stated that the principal types of toppling failure modes are block, flexural, mixed mode block-flexural, and secondary toppling. Furthermore, they stated that research of toppling failures has historically focused on block toppling, which is a failure mode associated with sliding and toppling of rock columns along a preexisting basal plane formed by a discontinuity dipping into the excavation. Little attention has been directed toward understanding the mechanisms of other failure modes or to the fact that, in practice, most toppling analyses (regardless of the actual mode) are undertaken using the classical method developed by Goodman and Bray (1976) for block toppling.

[1]Lecturer, Dept. of Structural Engineering and Dept. of Geological and Environmental Sciences, Ben-Gurion Univ. of the Negev, Beer-Sheva 84105, Israel (corresponding author). E-mail: michatse@bgu.ac.il

[2]Professor, Dept. of Geological and Environmental Sciences, Ben-Gurion Univ. of the Negev, Beer-Sheva 84105, Israel.

Note. This manuscript was submitted on November 7, 2007; approved on December 29, 2008; published online on February 23, 2009. Discussion period open until January 1, 2010; separate discussions must be submitted for individual papers. This paper is part of the ***Journal of Geotechnical and Geoenvironmental Engineering***, Vol. 135, No. 8, August 1, 2009. ©ASCE, ISSN 1090-0241/2009/8-1122–1129/$25.00.

The classical Goodman and Bray toppling analysis assumes that any single slab tends to overhang and is supported only by the passive resistance offered by its down-slope neighbors. Instability arises when the overturning moments, taken at the toe of a slab, are greater than the resisting moments. The underlying assumption in this approach is that rock slabs overhang due to their position on an inclined plane, the basal plane [Fig. 1(b)]. This assumption leads to the notion that there is a critical inclination angle for the basal plane, beyond which rotational instabilities occur. If the inclination of the basal plane is less than critical, the slope is considered safe against rotational failures. This approach, however, may not be suitable for failure mechanisms distinctly different from the commonly assumed block toppling mechanism.

An alternative view of this problem is that of eccentrically loaded sections. For a slender block resting on an inclined plane, the self-weight resultant can be decomposed into two components: normal and parallel to the inclined plane (Fig. 2). The normal component makes an angle ψ with the centerline of the block such that the load is eccentric. When the resultant lies outside the middle third of the rectangular section, eccentric loading will induce bending moments and consequently tensile stresses across the base. Since the base is typically a preexisting discontinuity of negligible tensile strength, such eccentric loading will result in opening across the discontinuity. The eccentricity of loading is a function of block slenderness and base inclination, h/b and ψ of the Goodman and Bray solution, respectively. The area of the section within which the action of the weight resultant does not induce bending moments at the base will be termed hereafter as the structural kernel of the section.

Similar loading conditions exist when the face of a slope overhangs over its toe (Fig. 3), such that the loading resultant is shifted from the centerline (Fig. 4). As discussed above in discon-

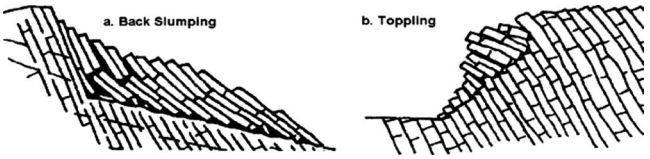

Fig. 1. Slender blocks on incline, typical geometry for rotational instabilities: (a) back slumping; (b) toppling (after Goodman and Kieffer 2000)

tinuous rock masses, which cannot resist tensile stresses, eccentric loading will induce opening across the discontinuities. The size and location of the section's kernel in overhanging slopes is determined by their face height (h) and inclination (α). A necessary condition for the forward rotational mode is the presence of a detachment plane, or tension crack, at the back of the overhanging slope. Such a detachment plane may be assumed if the rock mass is transected by vertical joints, either through the presence of high persistence tension cracks or by coalescence of less pervasive vertical joints and elimination of rock bridges (see Fig. 3). For this particular geometry, toppling may occur even when the basal discontinuities are horizontal and the block forming joints are vertical. Such slope geometries are common in sedimentary rock masses and are typically found in both natural and artificial environments, e.g., in hard-rock river banks where water flow erodes the base of the bank (Haviv et al. 2006), along coastal bluffs, and in quarried benches.

In this paper, an investigation of the kinematics of overhanging rock slopes and the structural constraints associated with this specific slope geometry is described. First a generalized rigid body analysis taking geometrical constraints into consideration is discussed, and thereafter a two-dimensional (2D) discontinuous deformation analysis (DDA) is presented; the DDA also accounts for the effects of secondary discontinuities. In addition, the DDA analysis is used for studying and dimensioning possible support schemes. The findings of both analyses are demonstrated by presenting an illustrative case study.

Geometric and Mechanical Considerations

In the discussion below, the following notation is used: slope height h, base length B, and face inclination angle α (see Fig. 3 for notation). The horizontal coordinate of the center of mass X_{CM} is given by

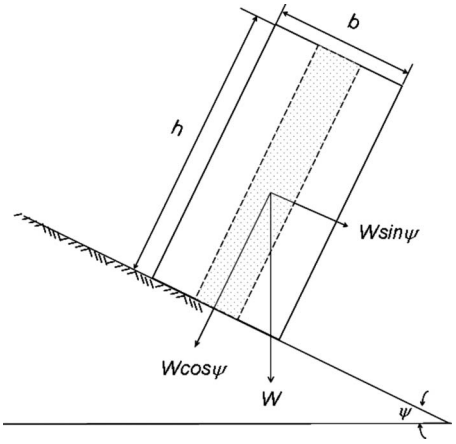

Fig. 2. Slender block on incline (after Goodman and Bray 1976). Shaded zone is section kernel.

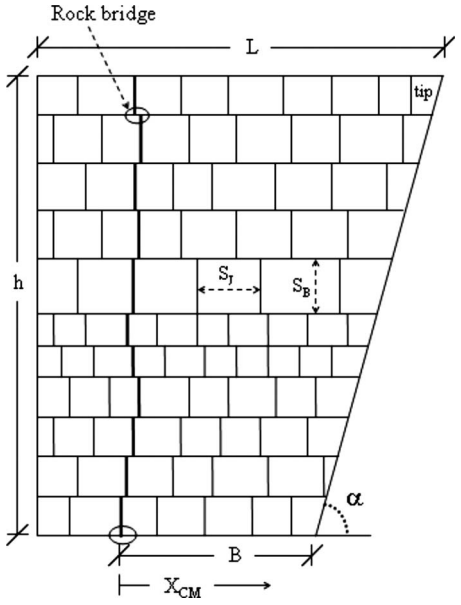

Fig. 3. Geometry and notations of overhanging rock face

$$X_{CM} = \frac{3B \cdot \tan\alpha + \frac{2}{3}h}{h(B+h)} \tag{1}$$

If the gravitational resultant acts within the section's kernel, i.e., $B/2 < X_{CM} < 2B/3$, then the base is under compression, although not uniform [Fig. 4(a)]. If $X_{CM} > 2B/3$ then the resultant action is applied outside the kernel, and bending moments will induce partial tension at the base [Fig. 4(b)]. Taking moments about the toe of the slope shows that as long as the resultant plots within the base of the slope, i.e., $X_{CM} < B$, the slope is safe against forward rotation. Note, however, that when the resultant line of action approaches B even slight horizontal perturbation, for example, due to external vibrations of seismic or blasting origin, may induce rotational instability. Once the resultant plots outside the base, the entire mass is unstable, and forward rotation is inevitable [Fig. 4(c)]. The unstable mass rotates about point O along a circular arch of a radius B [e.g., arch AA' in Fig. 4(c)], thus precluding reactions between the stable rock face and the back of the rotating mass. This will hold true only for gravitational loading; external perturbations, such as earthquake-induced horizontal accelerations, can possibly add a horizontal reaction, which with respect to point O will add an overturning moment.

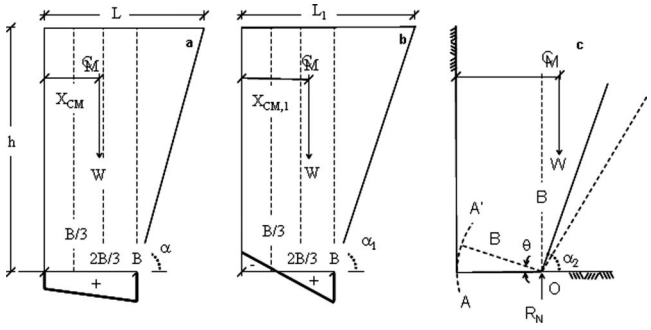

Fig. 4. Stress distribution at base of overhanging section: (a) centroid of mass within kernel; (b) centroid of mass external to kernel; and (c) rigid body diagram of forward rotating overhanging slope

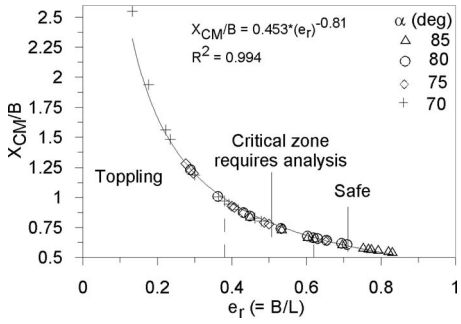

Fig. 5. Position of mass centroid (X_{CM}/B) as function of eccentricity ratio (e_r)

The eccentricity of loading can be assessed using the following geometric index: $e_r=B/L$, where $L=B+h/\tan\alpha$. A plot of the relative position of the center of mass X_{CM}/B, obtained analytically as a function of slope eccentricity ratio e_r—for slope heights of 35, 50, and 75 m and face angles of 85, 80, 70, and 65°—is presented in Fig. 5. A power law best describes the trend for X_{CM} with respect to the eccentricity ratio e_r (Fig. 5). On the basis of the obtained relationship the following limiting er values can be defined: for $e_r>0.62$, the block is safe; for $0.38<e_r<0.62$, the base of the block is partially in tension and possibly unsafe against toppling; and finally for $e_r<0.38$, toppling is inevitable. The ratio $e_r=0.38$ is therefore defined as the critical eccentricity ratio $e_{r,c}$. On the basis on the critical eccentricity ratio, a critical base depth (B_{crit}), beyond which rotation is impermissible by virtue of kinematics, may be defined. To find B_{crit} in terms of the obtainable field quantities h and α, the substitution $L=B_{crit}+h/\tan\alpha$ is used and the equation is solved for B_{crit}

$$B_{crit}=\frac{h}{1.6315\cdot\tan\alpha} \tag{2}$$

The critical base depth B_{crit} is plotted in Fig. 6 as a function of slope height h for different values of slope face inclination. Inspection of Fig. 6 reveals that in subvertical slopes, i.e., $\alpha=85°$, the critical detachment plane is near the face of the slope; for example, $B_{crit}=4$ m for $h=70$ m. For lower face inclinations, however, the critical detachment plane will be deeper within the rock mass; for example, $B_{crit}=17$ m at $h=70$ m and $\alpha=70°$. This observation explains the stability of steep and high rock slopes, even if eccentrically loaded failure is limited to the vicinity of the face and stable equilibrium is attained after a limited loss of rock mass. Based on Fig. 6, a simple "rule of thumb" is suggested for the critical distance between the tension crack and the toe

$$B_{crit}=\left\{0.05+0.05\cdot\left(\frac{85°-\alpha}{5}\right)\right\}\cdot h \tag{3}$$

The critical depth of the detachment plane is 5% of the slope height for a face inclination of 85°, rising by 5% for each 5° decrease of slope inclination.

With the distance to the critical tension crack being known, the length of the anchors may be designed such that the presence of the detachment plane becomes insignificant from a kinematical standpoint. By ensuring sufficient anchor length, the resultant can be made to plot inside the section kernel, thus eliminating rotational instabilities and the development of tensile stresses across the base of the slope.

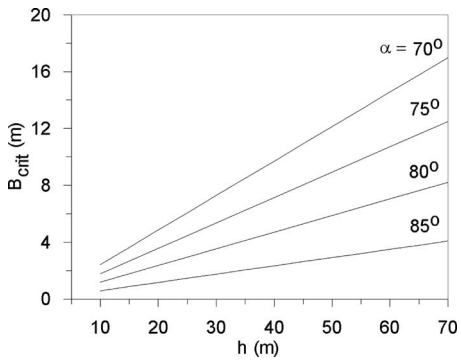

Fig. 6. Critical depth (B_{crit}) of detachment plane as function of slope height (h) and face inclination angle (α)

Overhanging Slope Stability in Discontinuous Rock Masses

Discontinuous rock masses have negligible resistance to tensile loads and therefore opening across the discontinuities is inevitable wherever tensile stresses are expected to develop in the discontinuous rock mass. In this paper, discontinuous deformation is modeled by using an implicit discrete element method—the DDA (Shi 1993).

Essentials of DDA Method

DDA is a discrete element method formulated using the minimum potential energy principal. DDA formulation of the blocks closely resembles the definition of a finite-element (FE) mesh. Here, a FE type problem is solved in which all elements are physically isolated blocks, bounded by preexisting discontinuities.

The displacements (u, v) at any point (x, y) in a block can be related in two dimensions to six displacement variables

$$[D_i]=(u_0 \quad v_0 \quad r_0 \quad \varepsilon_x \quad \varepsilon_y \quad \gamma_{xy})^T \tag{4}$$

where (u_0, v_0)=rigid body translations of a specific point (x_0, y_0) within a block; (r_0)=rotation angle of the block with a rotation center at (x_0, y_0); and ε_x, ε_y, and γ_{xy}=normal and shear strains of the block. For a two-dimensional formulation of DDA, the center of rotation (x_0, y_0) coincides with block centroid (x_c, y_c). Shi (1993) showed that the complete first-order approximation of block displacement takes the following form:

$$\begin{pmatrix} u \\ v \end{pmatrix}=[T_i][D_i]$$
$$=\begin{bmatrix} 1 & 0 & -(y-y_0) & (x-x_0) & 0 & (y-y_0)/2 \\ 0 & 1 & (x-x_0) & 0 & (y-y_0) & (x-x_0)/2 \end{bmatrix}[D_i] \tag{5}$$

This equation enables the calculation of displacements at any point (x, y) in the block when the displacements are given at the center of rotation and when the strains are known. By adopting first-order displacement approximation, each block is considered as a homogenously deformable (constant strain) element.

The local equations of equilibrium are derived using FE-style potential energy minimization, where individual blocks form a system of blocks through contacts between blocks and displace-

ment constraints that are imposed on a single block. For a block system defined by n blocks, the simultaneous equilibrium equations are

$$\begin{pmatrix} K_{11} & \cdots & K_{1n} \\ \vdots & \ddots & \vdots \\ K_{n1} & \cdots & K_{nn} \end{pmatrix} \begin{Bmatrix} D_1 \\ \vdots \\ D_n \end{Bmatrix} = \begin{Bmatrix} F_1 \\ \vdots \\ F_n \end{Bmatrix} \text{ or } [K]\{D\} = \{F\} \tag{6}$$

where K_{ij} $(i,j=1,2,\ldots,n)$=submatrices defined by the interactions of blocks i and j; D_i=displacement variables submatrix; and F_i=loading submatrix. In total, the number of displacement unknowns is the sum of the degrees of freedom of all the blocks.

The solution to the system of Eq. (4) is constrained by inequalities associated with block kinematics: the *no penetration—no tension* condition between blocks. The kinematic constraints on the system are imposed using the penalty method. The minimum energy solution is one with no tension or penetration. When the system converges to an equilibrium state, the energy of the contact forces is balanced by the penetration energy, resulting in inevitable, but very small, penetrations. The energy of the penetrations is used to calculate the contact forces, which are, in turn, used to calculate the frictional forces along the interfaces between blocks. Shear displacement along the interfaces is modeled using the Coulomb–Mohr failure criterion

Time integration is performed using an implicit, stepwise linear scheme, which is similar to the Newmark method, with the collocation parameters $\beta=\frac{1}{2}$ and $\gamma=1$.

Since its introduction, the DDA has been validated by a number of researchers using different techniques and for various engineering applications. A thorough review of the validation efforts is presented in McLaughlin and Doolin (2006).

Stability of Free Standing Overhanging Slopes

In this investigation, three slope heights, 35, 50, and 75 m are studied, where for each geometry, the eccentricity ratio e_r $(=B/L)$, is varied between 0.3 and 0.65. The modeled rock mass consists of a set of horizontal beds and a set of vertical joints, the intersection of which forms a blocky rock mass (Fig. 3). The aspect ratio of the individual blocks comprising the rock mass is set to $S_J/S_B>2$, where S_J and S_B=mean joint and bed spacing, respectively. Comprehensive numerical analyses reveal that for the slope geometries studied the rotational mode of failure is independent of the block aspect ratio, as long as $S_J/S_B\leqslant 1$. For smaller block aspect ratios, the mode of failure changes from mostly uniform rotation to falling of individual rock blocks, culminating in face raveling. The following intact rock parameters are used as input for numerical modeling: dry unit weight of 25 kN/m^3, Young's y modulus of 70 GPa, and a Poisson ratio of 0.25. The shear strength of the discontinuities is assumed purely frictional, with a peak friction angle of 41°. These values were chosen so as to represent a stiff sedimentary rock mass with clean, planar, and persistent discontinuities.

DDA time histories for the displacements at the tip of the slope are presented in Fig. 7 as a function of the eccentricity ratio e_r $(=B/L)$ for a slope height of 50 m. For $e_r<0.4$, the slope is unstable, as is evident from the ongoing deformation, whereas for $e_r>0.5$, the slope attains equilibrium after some initial deformation. The same trend was obtained for 35 and 70 m high slopes (results not shown here). Based on DDA, it can be concluded that the global stability of an overhanging rock slope is not affected by the presence of horizontal beds and vertical joints, provided that the shear strength along the discontinuities is not exceeded during forward rotation. Thus, the "rule of thumb" [Eq. (3)] can be assumed valid for horizontally bedded and vertically jointed rock masses as well.

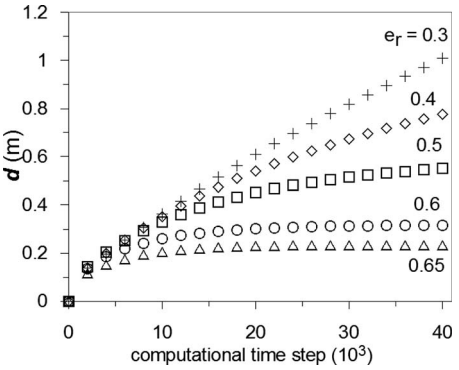

Fig. 7. DDA calculated time histories of slope tip displacement (d) as function of eccentricity ratio $e_r(=B/L)$ for slope height of 50 m

Reinforcement of Overhanging Rock Slopes

Discontinuous rock reinforcement can be modeled in DDA using spring elements (Shi 1993; Yeung 1993) of given stiffness and length to simulate the action of grouted rock bolts, dowels, or cable bolts. An example of rock bolt reinforcement modeling in the highly discontinuous rock slope foundations of King Herdod's palace at Masada was presented by Hatzor et al. (2004) for dynamic loading. Here, two different reinforcement schemes for overhanging rock slopes under static loading are considered: (1) full face support; and (2) partial face support up to a critical face height h_{crit}. In both cases, individual bolt length is adjusted such that the static end of each bolt is fixed beyond B_{crit}, thus eliminating the mechanical significance of the tension crack at the back.

Generally, bolt stiffness is given by: $k=AE/L_B$, where A =cross-sectional area of the bolt element; E=Young's modulus of the structural steel; and L_B=bolt length. For purposes of clarity, our results are presented in terms of an equivalent bolt diameter $\phi(")$, where in fact in the DDA model the stiffness of each bolt element is adjusted according to the actual element length used in each specific location.

In the partial face reinforcement scheme (2), reinforcement is applied from the bottom up such that the eccentricity ratio $(e_r=B/L)$ of the remaining unsupported part of the overhanging block increases. Consider, for example, a slope with an initially critical eccentricity ratio $e_{r,c}=0.38$. Without support, this block will undergo toppling. By installing reinforcement from the bottom up, the eccentricity ratio gradually increases from a critical value to some safer value, because the lower supported portion of the block is assumed fixed. At a certain reinforcement height, designated here as h_{crit}, the eccentricity ratio will eventually reach the stable value of $e_r=0.62$. Apparently, no further reinforcement should be necessary above that height. h_{crit} is readily found by Eq. (2) and the specific geometry of the problem at hand (see Fig. 8).

DDA forward modeling results for a 50 m high overhanging slope with an initial eccentricity ratio of $e_r=0.4$ are presented in Figs. 9(a and b). Fig. 9(a) presents a plot of the displacement vector of the face tip (Fig. 3) for the two reinforcement schemes both with the same bolt spacing $s=4$ m, and diameter $\phi=3$ in. In all simulations, a Young's modulus of 210 GPa is assumed for steel. The dashed lines represent the upper and lower displace-

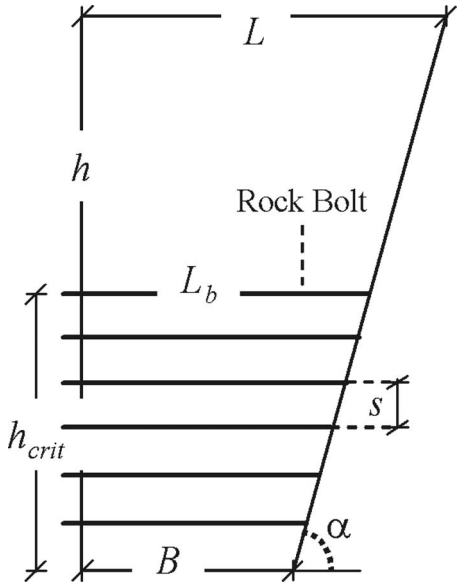

Fig. 8. Rock face reinforcement nomenclature

ment boundaries for unsupported slopes with eccentricity ratios of 0.4 and 0.65, respectively. Tip displacement with partial and full face support are marked by open diamonds and plus symbols, respectively. It is clearly evident that by supporting the slope up to h_{crit} the displacement of the tip is restricted to values typical to stable geometries. Furthermore, by supporting the entire face, no significant reduction in tip displacement is observed. Similar results (not shown here) were obtained for different bolt stiffness and spacing values. These results may indicate that partial support up to h_{crit} should suffice in overhanging slopes.

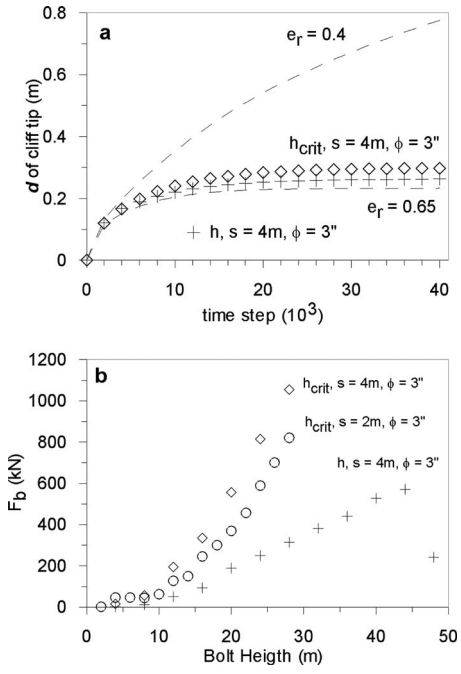

Fig. 9. DDA calculations of reinforced rock face: (a) displacement time histories; (b) bolt tensional forces; for slope height of 50 m and eccentricity ratio of e_r=0.4; h_{crit}=face support up to critical height; h=full face support; s=bolt spacing; ϕ=bolt equivalent diameter

To determine whether partial face support is indeed advantageous in overhanging slopes, the tensile loads developed in each reinforcing element (F_b) are considered. Tensile load distribution in the reinforcement elements for different support schemes are presented in Fig. 9(b). If partial support versus full face support schemes are considered for the same bolt spacing and diameter, then the full-face reinforcement scheme yields a maximum bolt tension of F_b=570 kN at the bolt located below the tip of the slope, 44 m above the toe, whereas for partial face support a maximum load of F_b=1,050 kN is developed at h_{crit}, 28 m above the toe of the slope. For comparison, at the same bolt location (28 m above the toe), the full face support scheme reduces the bolt load by a factor of three. Doubling the number of bolts in the partial face reinforcement scheme and reducing bolt spacing to s=2 m only slightly reduces bolt load distribution: the maximum bolt force in this configuration is F_b=820 kN for the bolt installed at h_{crit}.

In summary, if tip displacement alone is considered, then partial face reinforcement may seem adequate. However, when bolt load distribution is considered, the full-face support scheme seems to require lower individual bolt capacities, thus increasing the factor of safety against failure in individual bolts.

Case Study

In this section the stability of a quarried overhanging rock slope is studied and the applicability of the theoretical findings described above is demonstrated.

The studied overhang was formed due to quarrying activities in the early 1950s in Haifa, Israel. The general bearing of the cliff is SSW to azimuth 185°, but local variations in strike form large overhangs. Poor quarrying practices coupled with river bed erosion at the base of the cliff gave rise to large overhangs along the rim of the slope. Field observations at the top of the slope revealed open cracks, which strike parallel to the face, possibly suggesting ongoing slope deformation, particularly in areas where the cliff overhangs. A particular cross section, a 34 m high slope, the upper third of which extrudes some 11 m beyond the toe, constitutes the focus of this study (Fig. 10).

Rock Mass Characteristics

The rock is comprised of a bedded dolostone sequence. Bed thickness ranges between 5 and 150 cm. The rock mass is transected by four sets of subvertical joints. The strike of three sets is oblique to the face of the cliff, whereas the strike of the fourth is parallel to the excavation face. Mean orientation, dip, and spacing of discontinuities are presented in Table 1. The joints exhibit fresh, unaltered and uneven surfaces with a typical joint roughness coefficient value of 13. The joint wall compressive (JCS) strength is estimated at JCS=40 MPa (Schmidt hardness of 31). A residual friction angle of 37° is assumed for discontinuities based on tilt tests performed on saw-cut dolstone samples.

The subvertical joints are of limited persistence, while bedding planes are of "infinite" extent (Fig. 11). Since the face parallel joints are expected to have the most significant affect on overall cliff stability, they are modeled, similar to bedding, as infinite planes. The face parallel joint set (*J5* in Table 1) was detected on both sides of the slope segment studied, but naturally it cannot be detected in scan line surveys performed directly on the exposure. The face parallel set, where observed, seems to be very persistent, and in places openings across this joint set reach several tens of

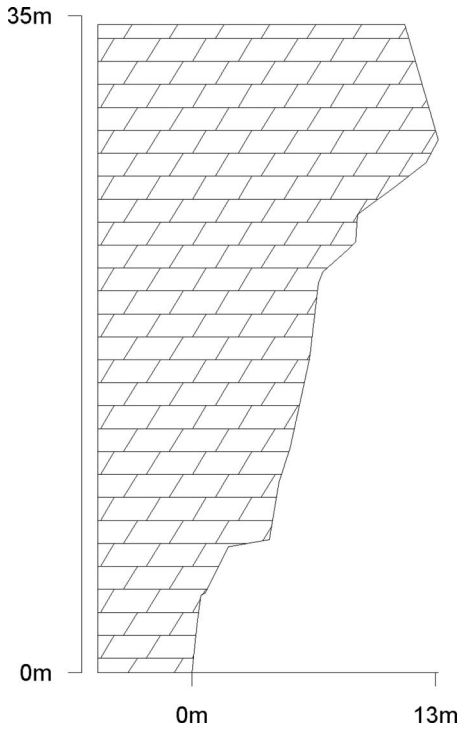

Fig. 10. Critical section of cliff studied

centimeters, indicating possible forward rotation of the entire slopes; this is in contrast to the other joint sets that terminate against bedding planes and do not exhibit any opening or shear deformation.

Key-Block Analysis

The key-block analysis is based on block theory (BT) introduced by Goodman and Shi (1985). BT is a topological analysis intended to identify the removable blocks within the rock mass augmented by limit equilibrium (LE) analysis for each removable block. The implementation of BT is geometrical, utilizing stereographic projection methods. First, the removable blocks are identified using Shi's theorem (Goodman and Shi 1985); each block is defined by a joint pyramid (JP) formed by the intersection of preexisting discontinuities and a free face (either natural or engineered); and then a three-dimensional LE based on the solution of Londe et al. (1970) is applied, and the factor of safety is computed for each of the removable blocks.

Hatzor and Feintuch (2005) proved that the probability of more than three joints (representative of three principal joint sets) passing through the same intersection in a jointed rock mass is zero. Therefore, the JP of interest consists of an intersection of

Table 1. Principal Joint Sets

Joint set	Dip (°)	Dip direction (°)	Spacing (m)
J1	7	272	0.8
J2	87	054	0.6
J3	88	184	0.9
J4	90	146	0.6
J5	90[a]	90[a]	?

[a]Inferred from field observations.

Fig. 11. Partial view of cliff studied; (inset): typical rock mass structure

three different joints. JPs of higher order are not likely to occur in the rock mass. Since there are four individual joint sets in the rock mass that participate in removable block formation, four different joint intersections, each with three different joint sets, should be considered for key-block analysis, the results of which are shown in Table 2.

LE analyses for each removable JP indicates that joint intersections 1, 2, and 3 yield a removable JP with very low factors of safety against sliding. The removable JP formed by joint intersection 3 has no mode and can therefore be excluded from further considerations. By using stereographic projection, it can be shown that each of the three removable JPs that have a low factor of safety has one line of intersection that plots very near the free surface. Such removable key blocks have been named "nonhazardous" (Hatzor 1993; Hatzor and Feintuch 2005), because, although removable, the volume of the block will be very small and consequently the associated risk minimal. This conclusion is supported by field evidence, where very few slender molds of failed key blocks were mapped along the face. Furthermore, by virtue of geometrical considerations, toppling of individual key blocks may also be ignored. Therefore, individual key-block failures, either in sliding or toppling mode, can be ruled out. The detected openings in the field across face-parallel tensile cracks may, however, imply that rotational instability of the entire overhanging slope block may presently be active.

Influence of Eccentric Loading on Global Slope Stability

The overhanging slope geometry results in eccentric gravity loading, as discussed in previous sections. The existence of persistent tensile cracks at the back of the slope enables forward slope rotation, due to the lack of tensile strength across the discontinuities. The size and location of the section's kernel, and the

Table 2. Block Theory Analysis Results

Joint intersection	Joint sets	Removable JP	Failure mode	F.S. ($\phi=37^0$)
1	$J_1J_2J_3$	100	$I_{2,3}$	0.18
2	$J_1J_2J_4$	100	$I_{2,4}$	0.04
3	$J_1J_3J_4$	010	No mode	—
4	$J_2J_3J_4$	010	$I_{3,4}$	0.04

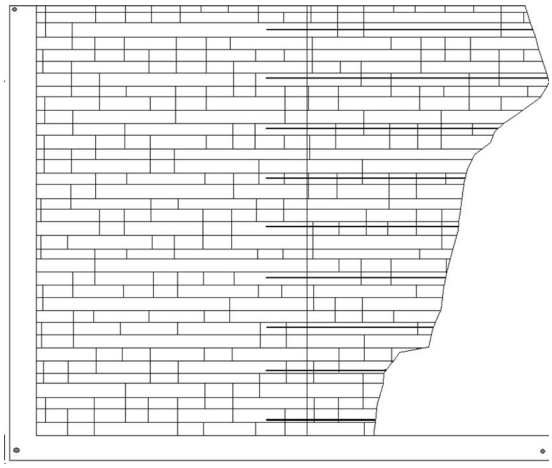

Fig. 12. DDA boundary domain of cliff studied with rock bolts

expected amount of rotation, are determined by the depth of the vertical tension crack and the height and the eccentricity ratio of the overhanging slope. As shown above, critical eccentricity is obtained when $e_r < 0.4$, which by virtue of Eq. (3) implies a tensile detachment joint at a depth of 8 m from the toe for the specified cliff geometry.

A slope reinforcement scheme is designed to accommodate eccentricity ratios lower than critical, down to $e_r = 0.3$, such that it will be capable of resisting overturning moments induced by tensile detachment planes that may exist at a depth of 5 m from the toe. Based on the results of the reinforcement analysis above, a bolt spacing pattern of $s = 4$ m is modeled for the entire height of the slope (Fig. 12). DDA displacements of slope tip and bolt loads are plotted in Figs. 13(a and b), respectively. It was found that complete slope stabilization is obtained with bolt diameter of $\phi = 2$ in. and above using the bolting pattern shown in Fig. 12. With

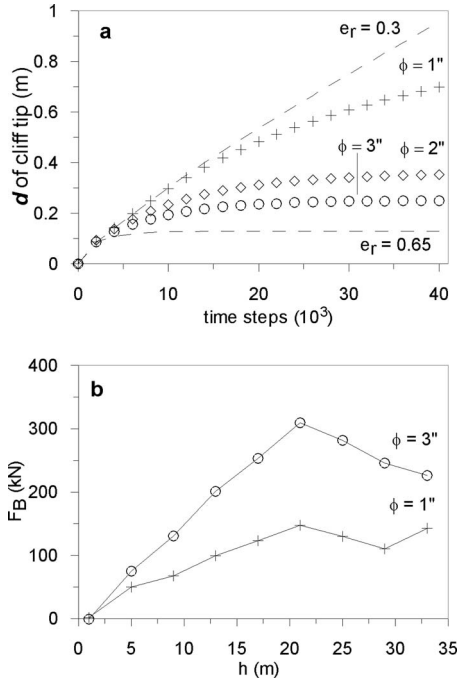

Fig. 13. DDA results for reinforced face of cliff studied: (a) displacement time histories of slope tip; (b) bolt forces

a bolt diameter of $\phi = 1$ in. slope displacements are never arrested, and the cliff is rendered unsafe. The maximum loads that develop in the bolts are 237 and 309 kN for bolt diameters of 2 and 3 in., respectively, which is well below the yield load of 500 kN assumed for twin strand cable bolts (Stillborg 1994).

Discussion

In this paper, the stability of overhanging rock slopes is studied using analytical geometry and numerical discontinuous deformation analysis. The stability of overhanging rock slopes is controlled primarily by two geometrical factors: (1) the presence of a vertical detachment plane behind the rock face; and (2) the eccentricity ratio of the slope determined by face geometry. While the face geometry can be measured readily in the field, the exact location of the detachment plane behind the face can only be assumed. It is, therefore, the location of the detachment plane that controls the global stability of overhanging rock slopes. As such, we consider it to be the prime factor of concern during stability analysis and support design.

The analyses presented are limited to a simple rock mass structure comprised of horizontal beds with vertical joints. Introducing bed and joint inclination will not affect the overall stability analysis as long as the friction angle along beds is not exceeded and the joint pyramids formed by the intersection of beds and joints form nonhazardous blocks (Hatzor and Feintuch 2005). In the presence of slender blocks, face raveling may be encountered, and when the basal planes are inclined, block toppling or block slumping (Goodman and Kieffer 2000) may be encountered. The eccentricity of loading, the location of the kernel, and consequently, the rotational instability are determined by the ratio between the slope base length B (or distance from toe to detachment plane) and the length of the top surface L (Fig. 3). These two geometrical quantities are interrelated through height h and face inclination α, such that $L = B + h/\tan\alpha$. The eccentricity of loading can also be defined by the ratio between the position of the center of mass X_{CM} and the base length B as follows:

1. When $X_{CM}/B = 0.5$, the section is concentrically loaded, and the slope is stable;
2. When $0.5 < X_{CM}/B < 0.66$, the section is eccentrically loaded. But the line of action of the gravitational resultant is within the section kernel—the slope may be considered safe, but local tensile deformations are expected behind the toe;
3. When $0.66 < X_{CM}/B < 1$, the section is eccentrically loaded, and the line of action is beyond the sections kernel—analysis is required to determine global slope stability; and
4. When $X_{CM}/B > 1$, the line of action plots outside the section, and global forward rotation is inevitable.

As a general rule, it is found that overhanging slopes can be assumed stable when the eccentricity ratio $e = B/L > 0.4$. This rule is confirmed by both kinematical and DDA analyses. This result was also confirmed by the FE method (FEM) analysis for a continuous two-dimensional section using STRAP 2D (Tsesarsky et al. 2005). It is interesting to note that for similar face geometries both DDA and FEM predict similar face displacements when no joints are modeled in DDA. Introduction of joints increases DDA displacements by an order of magnitude with respect to FE method results for a continuous body. However, the developed mode of failure remains unchanged. The discrepancies between the calculated displacements in the two methods are due to the governing constitutive relations implemented in each method. While in the continuous FE tensile stresses due to eccentric loads

are compensated for by vertical displacements at the base, in the discontinuous DDA these tensile stresses are compensated for by vertical displacements across bedding planes throughout the section height. The net displacement in DDA is the sum of individual displacements across all bedding planes in the mesh.

It was determined that optimal reinforcement in overhanging slopes should cover the entire height of the face. Reinforcing only the lower section of the face, for example, up to the critical height, where the eccentricity of loading is reduced to acceptable values, yields high bolt loads, which in some cases may exceed commercially available bolt capacities. Full face support yields lower individual bolt loads, typically by a factor of three for bolts at the same height. It can, therefore, be concluded that the apparent advantage of an economical reinforcement scheme is undermined by the relatively high demand on bolt capacity, which may ultimately result in unsatisfactory performance over time.

Conclusions

The stability of overhanging rock slopes is determined by the eccentricity of loading and kinematical feasibility. The eccentricity of loading is defined here using the eccentricity ratio $e_r = B/L$, where B=distance from slope toe to the tensile crack at the back; and $L = B + h\tan(\alpha)$=length of the top surface determined by the slope height (h) and face inclination (a).

The following guidelines for stability evaluation and support design are proposed:

1. An overhanging slope with an eccentricity ratio of $e_r > 0.62$ is safe against toppling failure;
2. An overhanging slope with an eccentricity ratio of $0.38 < e_r < 0.62$ is conditionally stable against toppling failure; support measures should be considered when approaching eccentricity ratio of 0.4;
3. An overhanging slope with eccentricity ratio of $e_r < 0.38$ is unstable against toppling failure; support should be installed immediately;
4. A support scheme for overhanging slope should be designed such that the eccentricity of loading X_{CM}/B is lowered to an acceptable minimum;
5. Full face support of the overhanging slope is recommended to reduce bolt loads to acceptable design values; and
6. DDA analysis shows that the overall stability of overhanging slopes is not compromised by the presence of horizontal beds and vertical joints.

Acknowledgments

This research was partially funded by the Office of Geotechnical and Foundation Engineering, Administration of Planning and Engineering, Ministry of Construction and Housing, Israel. Gen-hua Shi is thanked for implementing the bolt element in the DDA code version used in this research. Moshe Sokolowsky, Uzi Saltzman, and Itai Leviathan are thanked for discussions and cooperation in early stages of this work. Gony Yagoda is thanked for field survey and analysis of the structural data.

References

Adhikary, D. P., Dyskin, A. V., Jewell, R. J., and Stewart, D. P. (1997). "A study of the mechanism of flexural toppling failure of rock slopes." *Rock Mech. Rock Eng.*, 30(2), 75–93.

Evans, R. S. (1981). "An analysis of secondary toppling rock failures—The stress redistribution method." *Q. J. Eng. Geol.*, 14(2), 77–86.

Goodman, R. E., and Bray, J. W. (1976), "Toppling of rock slopes." *Proc., Specialty Conf. on Rock Engineering for Foundations and Slopes*, ASCE, New York, 201–234.

Goodman, R. E., and Kieffer, D. S. (2000). "Behavior of rock in slopes." *J. Geotech. Geoenviron. Eng.*, 126(8), 675–684.

Goodman, R. E., and Shi, G. H. (1985). *Block theory and its application to rock engineering*, Prentice-Hall, Englewood Cliffs, N.J.

Hatzor, Y. (1993). "The block failure likelihood—A contribution to rock engineering in blocky rock masses." *Int. J. Rock Mech. Min. Sci. Geomech. Abstr.*, 30(7), 1591–1597.

Hatzor, Y. H., Arzi, A. A., Zaslavsky, Y., and Shapira, A. (2004). "Dynamic stability analysis of jointed rock slopes using the DDA method: King Herod's Palace, Masada, Israel." *Int. J. Rock Mech. Min. Sci.*, 41(5), 813–832.

Hatzor, Y. H., and Feintuch, A. (2005). "The joint intersection probability." *Int. J. Rock Mech. Min. Sci.*, 42(4), 531–541.

Haviv, I., et al. (2006). "Amplified erosion above waterfalls and oversteepened bedrock reaches." *J. Geophysical Research-Earth Surface*, 111(4).

Kieffer, S. D. (1998). *Rock slumping—A compound failure mode of jointed hard rock slopes*, University of California Press, Berkeley, Calif.

Londe, P. F., Vigier, G., and Vormeringer, R. (1970). "Stability of rock slopes—Graphical methods." *J. Soil Mech. and Found. Div.*, 96(4), 1411–1434.

MacLaughlin, M. M., and Doolin, D. M. (2006). "Review of validation of the discontinuous deformation analysis (DDA) method." *Int. J. Numer. Analyt. Meth. Geomech.*, 30(4), 271–305.

Shi, G. H. (1993). *Block system modeling by discontinuous deformation analysis*, Computational Mechanics Press.

Stillborg, B. (1994). *Professional users handbook for rock bolting*, Pergamon Press .

Tsesarsky, M., Hatzor, Y. H., Leviathan, I., Saltzman, U., and Sokolowsky, M. (2005). "Structural control on the stability of overhanging, discontinuous rock slopes." *Proc., 40th U. S. Symp. on Rock Mechanics* (CD-ROM), Anchorage, Ala., Paper ARMA/USRMS 05–771.

Wittke, W. (1965). *Methods to analyze the stability of rock slopes with and without additional loading*, Springer, Vienna.

Yeung, M. R. (1993). "Analysis of a mine roof using the DDA method." *Int. J. Rock Mech. Min. Sci. Geomech. Abstr.*, 30(7), 1411–1417.